Photothermal deflection studies of GaAs epitaxial layers

Nibu A. George, C. P. G. Vallabhan, V. P. N. Nampoori, and P. Radhakrishnan

Photothermal beam deflection studies were carried out with GaAs epitaxial double layers grown on semi-insulating GaAs substrates. The impurity densities in thin epitaxial layers were found to influence the effective thermal diffusivity of the entire structure. © 2002 Optical Society of America
OCIS codes: 120.4290, 160.6000, 300.6430, 310.6870.

1. Introduction

The absorption of intensity modulated optical radiation by a sample leads to periodic heat generation, thereby causing excitation of thermal waves in the sample. Thermal wave physics is emerging as a valuable tool in the study of thermal properties of materials, especially in the semiconductor industry.[1–5] Among the various methods for investing these thermal waves the photothermal deflection (PTD) technique possesses some unique characteristics and advantages compared with the other approaches.[5–7]

The concept of light-beam deflection by thermally induced changes in the index of refraction of a medium has been known for a long time. However, only in did Boccara *et al.*[8] demonstrated the use of photothermal beam deflection as a valuable tool in material characterization. In subsequent years, theoretical and experimental contributions by Jackson *et al.*[9] in 1981, Aamodt and Murphy[10] in 1981, and Grice *et al.*[11] in 1983 formed a strong basis for this technique. The PTD technique is essentially based on detection of the refractive-index gradient associated with a temperature gradient. Absorption of optical radiation (the pump beam) results in the generation of thermal waves in a solid sample, which eventually generates a temperature gradient in a gas or a liquid that is in contact with the sample's surface. The refractive-index gradient associated with this temperature profile can be conveniently monitored by a second laser beam (the probe beam), which passes through the heated region, because the probe beam is deflected by the refractive-index gradient.

In the present paper we describe the use of the PTD technique for the thermal characterization of GaAs multilayer samples. Among the various experimental approaches to evaluating the thermal diffusivity of solids by use of PTD, the strategy that we used in the present investigation is measurement of the PTD signal phase as a function of pump–probe offset at a fixed modulation frequency.[6,12,13]

2. Theory

The PTD technique can be employed in various detection configurations for the investigation of solid samples.[6,7,14,15] Probe-beam deflection in the skimming configuration is one of the widely accepted and simple approaches among the PTD measurement schemes. A schematic representation of the probe-beam skimming configuration is shown as Fig. 1. In this configuration the solid sample is irradiated with a focused laser beam and the resultant refractive-index gradient generated in the coupling fluid (usually a liquid) that is in contact with the sample surface is monitored with a low-power probe beam passing through this gradient. In this scheme it is assumed that the temperature distribution in the coupling fluid located close to the sample surface is the same as that which is located at the sample surface. The probe beam propagating through the spatially varying refractive-index gradient suffers deflection from its normal path, and the amount of deflection is determined by a number of thermal and optical parameters of the solid sample.

For a Gaussian beam propagating through an inhomogeneous medium, most of the beam parameters can be deduced from the analysis made by Mandelis and Royce.[16] The propagation of a light beam

---

When this research was performed, N. A. George (nibu@ws.tn.tudelft.nl), C. P. G. Vallabhan, V. P. N. Nampoori, and P. Radhakrishnan were with the International School of Photonics, Cochin University of Science and Technology, Cochin 682022, India. N. A. George is now with the Department of Applied Physics, Thermal and Fluids Sciences Section, Delft University of Technology, The Netherlands.

Received 5 December 2001; revised manuscript received 27 March 2002.
0003-6935/02/245179-06$15.00/0

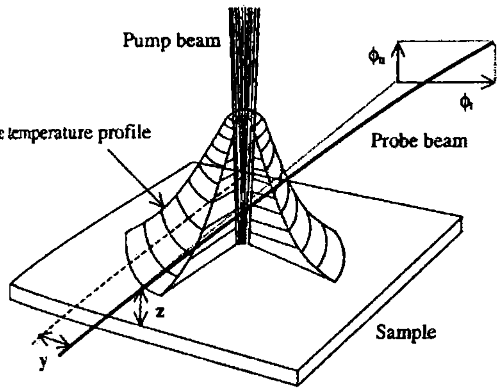

Fig. 1. Schematic diagram of the probe-beam skimming PTD configuration; y, z, the transverse and the vertical offsets, respectively.

through a spatially varying index of refraction is given by

$$\frac{\mathrm{d}}{\mathrm{d}s}\left(n_o \frac{\mathrm{d}r_o}{\mathrm{d}s}\right) = \nabla_{\perp} n(r, t), \qquad (1)$$

where r_0 is the perpendicular displacement of the beam from its original direction, n_0 is the uniform index of refraction, and $\nabla_{\perp} n(r, t)$ is the gradient of the index of refraction perpendicular to the ray path. Equation (2) can be integrated over the ray path:

$$\frac{\mathrm{d}r_o}{\mathrm{d}s} = \frac{1}{n_o}\int_{\text{path}} \nabla_{\perp} n(r, t)\mathrm{d}s, \qquad (2)$$

where s is the optical path length. Because the deflection is small, one can get the expression for the deflection, $\phi(t)$, as

$$\frac{\mathrm{d}r_o}{\mathrm{d}s} = \phi(t) = \frac{1}{n_o}\frac{\partial n}{\partial T}\int_{\text{path}} \nabla_{\perp} T(r, t)\mathrm{d}s, \qquad (3)$$

where $\nabla_{\perp} T(r, t)$ is the temperature gradient perpendicular to the ray path. Deflection $\phi(t)$ can be resolved into two components, ϕ_n and ϕ_t, where ϕ_n and ϕ_t are, respectively, the deflections normal and parallel to the sample surface. Let the probe beam make a transverse offset y with respect to the pump-beam axis and a vertical offset z with respect to the sample surface. The temperature field distribution that is due to the pump-beam absorption, obtained by solution of the heat diffusion equations in the sample as well as in the coupling fluid, leads to the evaluation of ϕ_t and ϕ_n as[13]

$$\phi_t = -\frac{1}{\pi n}\frac{\mathrm{d}n}{\mathrm{d}T}\int_0^{\infty} \sin(\delta y) A \exp(-\beta_0 z)\delta \mathrm{d}\delta$$
$$\times \exp(j\omega t), \qquad z > 0, \qquad (4)$$

$$\phi_n = -\frac{1}{\pi n}\frac{\mathrm{d}n}{\mathrm{d}T}\int_0^{\infty} \cos(\delta y) A \exp(-\beta_0 z)\beta_0 \mathrm{d}\delta$$
$$\times \exp(j\omega t) \qquad z > 0, \qquad (5)$$

where A is a complex integration constant, δ is a spatial Fourier-transformed variable, and $\beta_0 = (\delta^2 + j\omega/D_0)^{1/2}$, where D_0 is the thermal diffusivity of the coupling fluid.

Salazar *et al.* analyzed various experimental conditions and arrived at expressions that describe a linear relationship of the PTD signal phase as well as of the amplitude to various parameters such as pump–probe offset and height of the probe beam above the sample surface.[17] For $a = b = z = 0$, where a, b, and z are the pump-beam spot size. The probe-beam spot size, and the probe-beam height above the sample surface, there is a linear relationship between the phase of the transverse component of the probe-beam deflection and the pump–probe offset. This linearity is found to be valid for three different configurations: (1) probe-beam skimming configuration with the pump and the probe beams on the same side of the sample, (2) probe-beam skimming configuration with the pump and the probe beams on opposite sides of the sample, and (3) the probe beam passing through the sample. The experimental configuration used in the present study is of the first type. In this configuration the slope of the plot connecting the phase of the PTD signal and the pump-probe offset is given by

$$m = \frac{1}{\mu_s} = (\pi f/\alpha_s)^{1/2}. \qquad (6)$$

Practically, the condition $a = b = z = 0$ cannot be achieved, and finite values of a, b, and z may result in a change in slope, especially when the sample possesses low thermal diffusivity. But, for samples with moderately high thermal diffusivity, Eq. (6) holds for finite values of a, b, and z.[17,18]

3. Experimental

N-type and p-type GaAs thin films grown upon semi-insulating GaAs substrates were used in the investigation. The thin films were grown by the molecular beam epitaxial method (Technical University of Eindhoven, Eindhoven, The Netherlands). All of the samples contained two epitaxial layers. The sample structure together with the specifications of each layer, including the growth conditions and dopants, are given in Table 1. For convenience we have labeled the samples arbitrarily 1, 2, 3, and 4.

Continuous-wave laser emission at 488 nm from an argon-ion laser (Liconix 5000) was used as the pump beam. The laser beam had a $(1/e^2)$ diameter of 1.2 mm. In all the measurements a laser power of 50 mW ($\pm$0.5%) was used. Carbon tetrachloride (CCl_4), which is the most suitable and most commonly used coupling fluid in photothermal deflection studies, was used as the coupling fluid to the sample. The significant parameters that make CCl_4 a good coupling fluid in the PTD technique are its low thermal diffusivity, $\alpha = 7.31 \times 10^{-4}\ \mathrm{cm^2\ s^{-1}}$, and its very high rate of change of refractive index with respect to temperature, $(\mathrm{d}n/\mathrm{d}T) = 6.12 \times 10^{-4}\ K^{-1}$.[19]

A schematic view of the experimental setup is de-

Table 1. Structure, Properties, and Growth Conditions of the Doped GaAs Epitaxial Layers upon the Semi-Insulating GaAs Substrate

Sample	l (μm)[a]	n (cm^{-3})[b]	T (°C)[c]
1			
Si-doped GaAs (upper)	0.20	2.0×10^{18}	610
Si-doped GaAs (middle)	1.80	2.0×10^{18}	695
Semi-insulating GaAs (substrate)	400.0		
2			
Si-doped GaAs (upper)	0.20	2.0×10^{16}	610
Si-doped GaAs (middle)	2.80	2.0×10^{16}	695
Semi-insulating GaAs (substrate)	400.0		
3			
Si-doped GaAs (upper)	0.25	3.6×10^{14}	580
Si-doped GaAs (middle)	10.0	3.6×10^{14}	630
Semi-insulating GaAs (substrate)	400.0		
4			
Be-doped GaAs (upper)	0.20	2.0×10^{18}[d]	610
Be-doped GaAs (middle)	1.80	2.0×10^{18}[d]	695
Semi-insulating GaAs (substrate)	400.0		

[a]Thickness of layer.
[b]Electron concentration.
[c]Substrate temperature at which the layers are grown.
[d]Hole concentration (p).

picted in Fig. 2. The sample was placed horizontally at the bottom of a quartz cuvette with dimensions 10 mm × 10 mm × 40 mm, and CCl_4 is added to the cuvette to a height of ~10 mm above the sample surface. The argon-ion laser beam was focused upon the sample surface by a convex lens of 20-cm focal length. The pump-beam spot size at the sample surface was estimated to be 102 μm. The mirror and the lens (L_1, Fig. 2) were fixed on an xy translator, and the translator is positioned in such a way that the center of the mirror, the lens, and the cuvette are in a vertical line, the z axis. In this experimental arrangement one can accurately vary the pump-

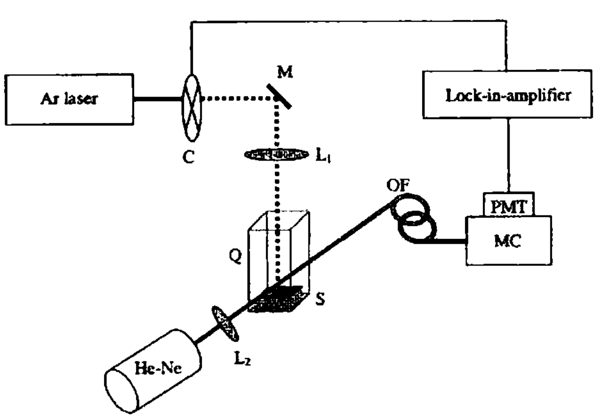

Fig. 2. Schematic view of the experimental setup: M, mirror; C, chopper; L_1, L_2, lenses; Q, cuvette; S, sample; OF, optical fiber; MC, monochromator; PMT, photomultiplier tube.

beam's position on the sample along the x direction [illegible] simply moving the translator in the x direction. [illegible] mechanical chopper (Stanford Research Systems Model SR540) was placed in the pump-beam path [illegible] modulate the pump beam's intensity at the desired frequency.

A 3-mW He–Ne laser (Spectra-Physics) emitting [illegible] 632.8 nm was used as the probe beam to detect [illegible] strength of the refractive-index gradient generated [illegible] CCl_4. The probe laser beam had a Gaussian profile with a ($1/e^2$) diameter of 800 μm and was focused [illegible] a convex lens of 10-cm focal length. The probe beam's spot size at the point where it crosses [illegible] pump beam was estimated to be 101 μm. The probe laser was arranged such that it just skims through the surface of the sample, and it propagates in a direction (y axis) orthogonal to that of the pump beam (z axis).

A plastic fiber with a circular core of 1-mm diameter was used as a position-sensitive detector to monitor the periodic deflection of the probe beam. [illegible] end of the fiber was firmly fixed upon an xyz translator at a distance of 15 cm from the sample. [illegible] other end of the fiber was coupled to a 0.25-m monochromator (McPherson) tuned to the probe beam wavelength. A photomultiplier tube was coupled [illegible] the exit slit of the monochromator. The output [illegible] the photomultiplier tube was fed to a dual-phase digital lock-in-amplifier (Stanford Research Systems Model SR830) through an impedance-matching circuit. The entire experimental setup was laid out [illegible] a moderately vibration-isolated table to protect [illegible] system from ambient vibrations. Measurements were carried out at a pump-beam modulation frequency of 10.6 Hz, and the distance between [illegible] probe beam height and the sample surface was kept as small as possible to produce a nondiffracted (from the sample edge) probe beam at the detector.

4. Results and Discussion

Measurements were carried out by irradiation of [illegible] thin-film sides as well as of the substrate sides of [illegible] samples. In the present experiment the probe beam, the position-sensitive detector, and the sample were firmly fixed at specific positions and the pump beam irradiation site on the sample surface was varied across the probe beam. A typical variation of [illegible] signal phase with the pump–probe offset for sample [illegible] when the semi-insulating GaAs substrate side is [illegible] ing the pump beam is shown in Fig. 3. The [illegible] mum in the phase plot corresponds to zero offset. Identical signal profiles were observed for the [illegible] strates of other samples also. From the slope [illegible] either side of the plot the thermal diffusivity of [illegible] substrate was evaluated by use of the relation given [illegible] Eq. (6). The measured values of α, calculated from the average of the two slopes, are listed in Table [illegible] Almost identical α values obtained for the substrates of all the four samples indicate that the epitaxial layers grown upon the other surfaces of the substrates had [illegible] significant influence on the PTD signal generated from the substrate. The literature values of α of GaAs [illegible]

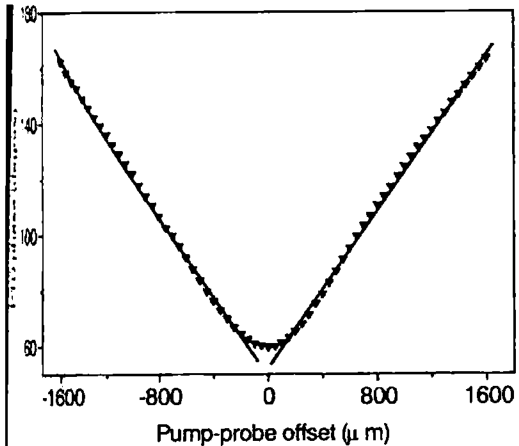

Fig. 3. Variation of PTD signal phase with pump–probe offset for sample 1 (substrate-side illumination).

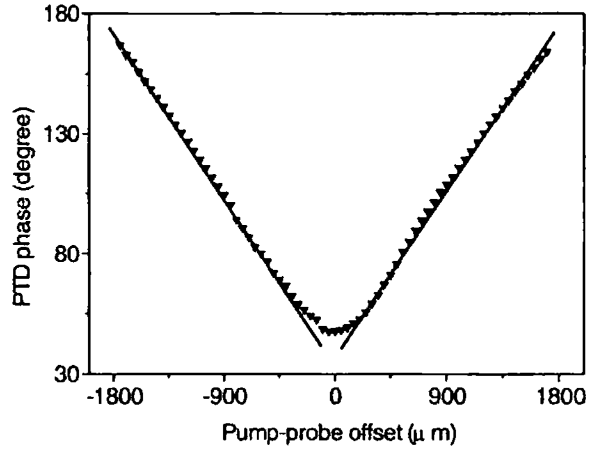

Fig. 4. Variation of PTD signal phase with pump–probe offset for sample 1 (film-side illumination).

in the range 0.2–0.36 $cm^2\ s^{-1}$,[14,20–25] and the experimentally observed values also fall within this range. The wide range of α values reported in the literature is due to the large variation of thermal transport properties of semiconductor materials with the growth conditions, defects, etc. In the case of a semi-insulating semiconductor, the free-carrier density is low and here, similarly to the heat conduction in dielectrics, the phonons make the main contribution to heat transport in these materials.[25,26]

Figure 4 shows the variation of PTD signal phase with the pump–probe offset for sample 1 when the thin-film side is facing the pump beam. Again, the thermal diffusivities of the films were evaluated from the slope of the plot, and the average values of the measured α are listed in Table 2. To explain the interesting results obtained from the epitaxial layers we need to recollect some of the fundamental facts regarding heat conduction in semiconductors. In semiconductor samples, in addition to the pure thermal wave effect, electronic diffusion and carrier recombination, may also contribute to the PTD signal. The pure thermal wave component of the PTD signal arises from the instantaneous intraband electron–phonon interaction and the subsequent phonon transport. For an extrinsic semiconductor, in addition to the contribution by free carriers, a nonradiative recombination of the photoexcited carriers that have diffused through the sample may also contribute

Table 2. Thermal Diffusivity Values of GaAs Multilayers Evaluated from the Photothermal Beam Deflection Measurements

	Thermal diffusivity α ($cm^2\ s^{-1}$)	
Sample Number	Film-Side Illumination	Substrate-Side Illumination
1	0.193	0.212
2	0.187	0.212
3	0.165	0.210
4	0.160	0.206

to the heat transport. Fournier *et al.* made a rigorous theoretical and experimental analysis in this regard and proved that, at very low frequencies, i.e., when $\omega\tau \ll 1$, only the pure thermal wave component contributes to the PTD signal; consequently the signal's behavior (both amplitude and phase) is characterized by the thermal diffusivity of the sample.[27] Here, $\omega = 2\pi f$, where f is the pump beam's modulation frequency and τ is the photoexcited carrier recombination lifetime. When the pump beam's modulation time scale is much shorter than τ, however, i.e., when $\omega\tau \gg 1$, the contribution from the pure thermal wave component drops off, and recombination processes now dominate the PTD signal. In this regime the signal behavior is characterized by electronic diffusivity. Usually, τ for n-type GaAs is of the order of microseconds, and for p-type GaAs it is as low as nanoseconds.[20–22] Hence at a modulation frequency of 10.6 Hz the contributions from photoexcited carrier recombination are expected to be negligible. Furthermore, it is clear from Fig. 4 that Eq. (6) holds in the case of epitaxial layers also, in agreement with the previous statement that the contribution from photoexcited carrier recombination is negligible.

The excitation photon energy, 2.54 eV, is much greater than the bandgap energy of GaAs (1.43 eV), and the entire energy is absorbed at the surface (~1 μm) of the epitaxial layer itself. Consequently the samples are optically opaque at the excitation wavelength. Moreover, the fact that the entire energy is absorbed at the surface of the sample implies that heat is generated in the surface epitaxial layer but propagates through the entire structure. Nevertheless, the decrease of α values of the epitaxial layers compared with the bulk diffusivity value suggests some interesting but complex heat transport mechanisms in these samples. The increase in the number of scattering centers that resulted from doping of GaAs with either Si or Be and the consequent reduction of the phonon mean free path do not seem to be the only reasons for the noticeable reduction in the diffusivity values of the epitaxial layers. Recently a number of research papers reported the experimental observation of substantial reduction (as much as 50%) in lattice thermal conductivity in semiconductor thin films, especially when the thin-film thickness was of the order of the phonon's mean free path.[20,28–31] But the exact values of the phonon's mean free path of the samples investigated here are not available for detailed analysis. According to the kinetic theory the phonon's mean free path in the bulk sample Λ_{bulk} can be evaluated from the relation

$$\Lambda_{\text{bulk}} = 3k_{\text{bulk}}/C\nu, \tag{7}$$

where k_{bulk} is the bulk thermal conductivity, C is the volumetric heat capacity, and ν is the speed of sound in the material. For bulk GaAs, $k_{\text{bulk}} = 0.46\ \text{W/(cm/°C)}$, $C = 0.33\ \text{J(g/°C)}$, and $\nu \approx 4.0 \times 10^5$ cm/s, which lead to the estimation of a phonon mean free path of approximately 100 nm.[20–22] This value is smaller than those of the surface layer thicknesses 200 and 250 nm, of the samples. However, the estimated value of the phonon's mean free path need not be strictly true, because there is a large discrepancy between the experimentally observed value of the phonon's mean free path and that evaluated theoretically; hence it is hard to analyze the observed thermal diffusivity data without knowing the exact value of Λ_{bulk}. For example, in a recent paper Ju and Goodson measured the effective phonon mean free path in Si as 300 nm, whereas that evaluated by the kinetic theory is only 43 nm.[28] But an important point to be mentioned is that the thicknesses of the thin films are too small compared with the thermal diffusion length and hence the tabulated thermal diffusivity value may be the effective diffusivity of the thin films and that of the substrate. However, a general conclusion that can be drawn from the tabulated thermal diffusivity values is that, for samples 1–3, all doped with Si, the trend is for a decrease in thermal diffusivity with a decrease in doping density and an increase in thickness of the second (under) epitaxial layer. Also, for sample 4, which is doped with Be, the diffusivity value is smaller than that of the corresponding n-type sample (sample 1).

This study is supported by the Netherlands University Federation for International Collaboration, The Netherlands. The authors thank J. H. Wolter and J. E. M. Haverkort, Technical University of Endhoven, Eindhoven, The Netherlands, for providing the sample.

References

1. D. O. Thompson and D. E. Chimenti, eds., *Review of Progress in Quantitative Nondestructive Evaluation* (Plenum, New York, 1985), Vol. 4B.
2. C. Wang and A. Mandelis, "Purely thermal-wave photopyroelectric interferometry," J. Appl. Phys. **85**, 8366–8377 (1999).
3. C. Christofides, F. Diakonos, A. Seas, C. Christou, M. Nestoros, and A. Mandelis, "Two-layer model for photomodulated thermoreflectance of semiconductor wafers," J. Appl. Phys. 1713–1725 (1996).
4. R. E. Wagner and A. Mandelis, "Nonlinear photothermal ulated optical reflectance and photocurrent phenomena crystalline semiconductors: theoretical," Semicond. Technol. **11**, 289–299 (1996).
5. A. Mandelis, Ed., *Photoacoustic and Thermal Wave Phen ena in Semiconductors* (North-Holland, New York, 1987).
6. J. A. Sell, *Photothermal Investigations of Solids and* (Academic, Boston, Mass., 1989).
7. P. Hess and J. Pelzl, eds., *Photoacoustic and Photothe Phenomena* (Springer-Verlag, Berlin, 1988).
8. A. C. Boccara, D. Fournier, and J. Badoz, "Thermo-o spectroscopy: detection by the 'mirage effect,'" Appl. Lett. **36**, 130–132 (1980).
9. W. B. Jackson, N. M. Amer, A. C. Boccara, and D. Four "Photothermal deflection spectroscopy and detection," Opt. **20**, 1333–1344 (1981).
10. L. C. Aamodt and J. C. Murphy, "Photothermal measurem using a localized excitation source," J. Appl. Phys. **52**, 4914 (1981).
11. K. R. Grice, L. J. Inglehart, L. O. Favro, P. K. Kuo, and Thomas, "Thermal wave imaging of closed cracks in op solids," J. Appl. Phys. **54**, 6245–6255 (1983).
12. P. K. Kuo, M. J. Lin, C. B. Reyes, L. D. Favro, R. L. Th D. S. Kim, S. Zhang, L. J. Inglehart, D. Fournier, A. C. Bo and N. Yacoubi, "Mirage effect measurement of thermal sivity. I. Experimental," Can. J. Phys. **64**, 116 (1986).
13. M. Bertolotti, R. L. Voti, G. Liakhou, and C. Sibilia, "O photodeflection method applied to low thermal-diffus measurements," Rev. Sci. Instrum. **64**, 1576–1583 (199
14. D. Bicanic, ed., *Proceedings of Seventh International To Meeting on Photoacoustic and Photothermal Phen* (Springer, Berlin, Germany, 1992).
15. M. Bertolotti, G. L. Liakhou, R. L. Voti, S. Paolini, an Sibilia, "Analysis of the photothermal deflection techniq the surface reflection scheme: theory and experim J. Appl. Phys. **83**, 966–982 (1998).
16. A. Mandelis and B. S. H. Royce, "Fundamental-mode beam propagation in optically inhomogeneous electroche media with chemical species concentration gradients," Opt. **23**, 2892–2901 (1984).
17. A. Salazar and A. S. Lavega, "Thermal-diffusivity meas ments using linear relations from photothermal wave ex ments," Rev. Sci. Instrum. **65**, 2896–2900 (1994).
18. A. Salazar, A. S. Lavega, and J. Fernandez, "Ther diffusivity measurements in solids by the mirage techn experimental results," J. Appl. Phys. **69**, 1216–1223 (19
19. S. E. Bialkowski, *Photothermal Spectroscopy Method Chemical Analysis* (Wiley, New York, 1996).
20. G. Chen, C. L. Tien, X. Wu, and J. S. Smith, "Ther diffusivity measurement of GaAs/AlGaAs thin-film st tures," J. Heat. Transfer **116**, 325–331 (1994).
21. M. E. Levinshtein, S. L. Rumyantsev, and M. Shur, *Handbook Series on Semiconductor Parameters* (World Scien tific, London, 1996).
22. S. Adachi, *Physical Properties of III–V Semiconductor Com pounds* (Wiley, New York, 1992).
23. A. Dargys and J. Kundroats, *Handbook on Physical Prope of Ge, Si, GaAs, and InP* (Science and Encyclopedia Publis Vilnius, Lithuania, 1994).
24. M. Soltanolkotabi, G. L. Bennis, and R. Gupta, "Tempera dependence of the thermal diffusivity of GaAs in the K range measured by the pulsed photothermal displa technique," J. Appl. Phys. **85**, 794–798 (1999).
25. C. M. Bhandari and D. M. Rowe, *Thermal Conduction in conductors* (Wiley, New York, 1988).

A. C. Willardson and C. Beer, eds., *Semiconductors and Semimetals* (Academic, New York, 1988).

D. Fournier, C. Boccara, A. Skumanich, and N. M. Amer, "Photothermal investigation of transport in semiconductors: theory and experiment," J. Appl. Phys. **59**, 787–795 (1986).

Y. S. Ju and K. E. Goodson, "Phonon scattering in silicon films with thickness of order 100 nm," Appl. Phys. Lett. **74**, 3005–3007 (1999).

29. G. Chen, "Phonon wave heat conduction in thin films and superlattices," J. Heat Transfer **121**, 945–953 (1999).
30. T. F. Zeng and G. Chen, "Phonon heat conduction in thin films: impacts of thermal boundary resistance and internal heat generation," J. Heat Transfer **123**, 340–347 (2001).
31. M. Asheghi, Y. K. Leung, S. S. Wong, and K. E. Goodson, "Phonon-boundary scattering in thin silicon layers," Appl. Phys. Lett. **71**, 1798–1800 (1997).